Fractional Boundary Element Solution of Three-Temperature Thermoelectric Problems

Mohamed Fahmy (maselim@uqu.edu.sa)
Umm Al-qura University
Mohammed Almehmadi
Umm Al-qura University
Ayesha Sohail
COMSATS University Islamabad
Fahad Al Subhi
Umm Al-qura University

Research Article

Keywords: Boundary element method, Fractional-order, Three-temperature, Generalized thermoelasticity, Functionally graded magnetic thermoelectric structures

Posted Date: February 18th, 2022

DOI: https://doi.org/10.21203/rs.3.rs-1351104/v1

Fractional Boundary Element Solution of Three-Temperature Thermoelectric Problems

Mohamed Abdelsabour Fahmy[1, 3], **Mohammed M. Almehmadi**[2, *], **Fahad M. Al Subhi**[4] **and Ayesha Sohail**[5]

[1] Department of Mathematics, Jamoum University College, Umm Al-Qura University, Alshohdaa 25371, Jamoum, Makkah, Saudi Arabia; maselim@uqu.edu.sa

[2] Department of Mathematical Sciences, Faculty of Applied Sciences Umm Al-Qura University, Makkah 24381, Saudi Arabia; s44285534@st.uqu.edu.sa

[3] Faculty of Computers and Informatics, Suez Canal University, New Campus, 41522 Ismailia, Egypt; mohamed_fahmy@ci.suez.edu.eg

[4] Department of Mathematics, Jamoum University College, Umm Al-Qura University, Alshohdaa 25371, Jamoum, Makkah, Saudi Arabia; fmsobhi@uqu.edu.sa

[5] Department of Mathematics, Comsats University Islamabad, Lahore Campus, 54000, Pakistan; ayeshasohail81@gmail.com

* Correspondence: maselim@uqu.edu.sa Tel.: 00966537930306

Abstract: The primary goal of this article is to propose a new fractional boundary element technique for solving nonlinear three-temperature (3T) thermoelectric problems. Analytical solution of the current problem is extremely difficult to obtain. To overcome this difficulty, a new numerical technique must be developed to solve such problem. As a result, we propose a novel fractional boundary element method (BEM) to solve the governing equations of our considered problem. Because of the advantages of the BEM solution, such as the ability to treat problems with complicated geometries that were difficult to solve using previous numerical methods, and the fact that the internal domain does not need to be discretized. As a result, the BEM can be used in a wide variety of thermoelectric applications. The numerical results show the effects of the magnetic field and the graded parameter on thermal stresses. The numerical results also validate the validity and accuracy of the proposed technique.

Keywords: Boundary element method, Fractional-order; Three-temperature, Generalized thermoelasticity, Functionally graded magnetic thermoelectric structures

NOMENCLATURE

β_{ij}	Stress–temperature coefficients	C_{ijkl}	Constant elastic moduli

δ_{ij}	Kronecker delta $(i,j=1,2)$	E_i	Electric field vector
ε_{ij}	Strain tensor	e	$=\varepsilon_{kk}$ Dilatation
ε_{ijk}	permutation symbol	F_i	Mass force vector
ϵ_{ij}	Micro-strain tensor	$\mathbb{f}_{il}$	Permittivity tensor
λ	Tractions	H_i	Magnetic field intensity
μ_0	Magnetic permeability	H_0	Constant magnetic field
π_0	Peltier coefficient	J_i	Electric density vector
ρ	Density	$\mathbb{K}_\alpha$	Conductive coefficients
σ_{ij}	Stress tensor	k_0	Seebeck coefficient
σ_0	Reference stress	m	Functionally graded parameter
$\widetilde{\sigma_0}$	Electric conductivity	P	Total energy of unit mass
τ	Time	p	Pore pressure
τ_0,τ_1,τ_2	Relaxation times	T_α	Temperature functions
Å	Unified parameter	$T_{\alpha 0}$	Reference temperature
a	Fractional order parameter	u_i	Displacement vector
B_i	Magnetic strength components	$\mathbb{W}_{\mathrm{ei}}$	electron-ion energy coefficient
c_α	Specific heat capacities	$\mathbb{W}_{\mathrm{er}}$	electron-phonon energy coefficie

Introduction

Utilizing initial conditions and boundary conditions at m and Max Planck proposed the quantum theory of electromagnetic radiation in 1900, and Albert Einstein proposed the concept of photons and phonons in 1905 and 1907 to explain why temperature varies with the specific heat of solid crystals. A phonon is a quantum of vibrational mechanical energy produced by a lattice of oscillating atoms, where the thermal energy of the atoms causes the lattice to vibrate. This generates compression mechanical waves, which carry heat and sound through the anisotropic material. The careful study of phonons is an important part of solid-state physics because it is important for many thermal and acoustic properties of solids, as well as a variety of low- and high-temperature superconductive technologies.

Many bodies undergo significant changes in their properties as a result of the application of an electric or magnetic field, allowing for the profitable application of this fact in technological applications. The development of electrorheological and magnetic fluids has piqued the interest of many people due to their potential applications in clutches, actuators, shock absorbers, valves, and exercise equipment, to name a few. Field dependent solids, also known as electro-active elastomers, were recently developed by infusing elastomers with electrorheological fluids or embedding them with electrically conducting particles. Magneto-active elastomers, on the other hand, were created by encapsulating elastomers with magnetically responsive particles. Such field dependent solids have potential applications due to the change in structure and the resulting effect on the elasticity and compliance of the material, such field dependent solids have potential applications in a wide range of applications.

Knopoff [1] and Chadwick [2], followed by Kaliski and Petykiewicz [3], pioneered the magnetoelasticity foundations. Magnetic theory development and application were previously solely based on magnetic experiments. Because of the rapid development of high-performance computational methods and computer hardware, efficient and accurate computational methods for modeling and simulation of real

magnetic experiments have been used, particularly when the magnetic experiment is difficult, dangerous, or expensive.

Magnetorheological fluids (MR) are a type of smart material whose rheological properties can be rapidly altered by applying a magnetic field. Rajagopal and Ru zicka [4] developed governing equations for the motion of electrorheological fluids that account for the complex interaction of thermomechanical and electro-magnetic fields. Brigadnov and Dorfmann [5] investigated the entire system of equations as well as the Clausius–Duhem inequality for isotropic MR fluids flowing in an electro-magnetic field. Dorfmann and Ogden [6] have described the equations governing the deformation of magneto-sensitive (MS) elastic materials, with special reference to elastomers whose mechanical characteristics can be rapidly modified by applying a magnetic field.

These "smart materials" are frequently composed of micron-sized ferrous particles dispersed in an elastomeric matrix. Based on Carlson and Jolly's experimental results, the fundamental system of constitutive equations for MS Cauchy-elastic solids was then established using a phenomenological method [7]. Magnetorheological elastomers (MREs) are a class of materials composed of a rubber matrix filled with magnetizable particles, often sub-micron sized iron particles, according to Rajagopal [8], Rigbi and Jilkén [9], and Ginder [10]. The magnetoelastic coupling properties of these materials have piqued the interest of researchers. MREs are finding an increasing number of technical applications due to their high magnetoelastic coupling response, necessitating proper theoretical explanations, which is the goal of [11].

The interaction between magnetic and strain fields in a thermoelastic solid is receiving increased attention due to its numerous applications in geophysics, plasma physics, and other fields. All of the articles cited above assumed that interactions between the two fields occur via Lorentz forces appearing in equations of motion and a term entering Ohm's law and representing the electric field created by the velocity of a material particle traveling in a magnetic field. In these investigations, the heat equation under consideration is typically the uncoupled or coupled theory, rather than the generalised one. Ezzat and Awad developed a model of micropolar generalised magneto-thermoelasticity based on modified Ohm's and Fourier's laws [12]. In the literature, several fractional-order models have been investigated for various applications. There is no general analytical solution due to the computational difficulty of solving complex fractional nonlinear thermoelasticity problems. Numerical methods, including the BEM, should be used to solve such problems. Different three-temperature theories have been investigated in the context of micropolar-thermoelasticity [13], carbon nanotube fiber reinforced composites [14], micropolar piezothermoelasticity [15], Micropolar Magneto-thermoviscoelasticity [16] and Magneto-thermooviscoelasticity [17] Also, Fahmy introduced new boundary element models for bioheat problems [18], micropolar composites with temperature-dependent problems [19], Generalized Porothermoelastic Problems [20] and Size-Dependent thermopiezoelectric Problems [21]

In this paper, we presented a new fractional order theory of functionally graded magnetic thermoelectric materials. This theory's application to three-temperature nonlinear generalized thermoelasticity is solved using boundary element analysis. The numerical results demonstrate the effects of a magnetic field and a graded parameter on thermal stresses in FGMTM. The numerical results also confirm the validity and accuracy of the proposed technique.

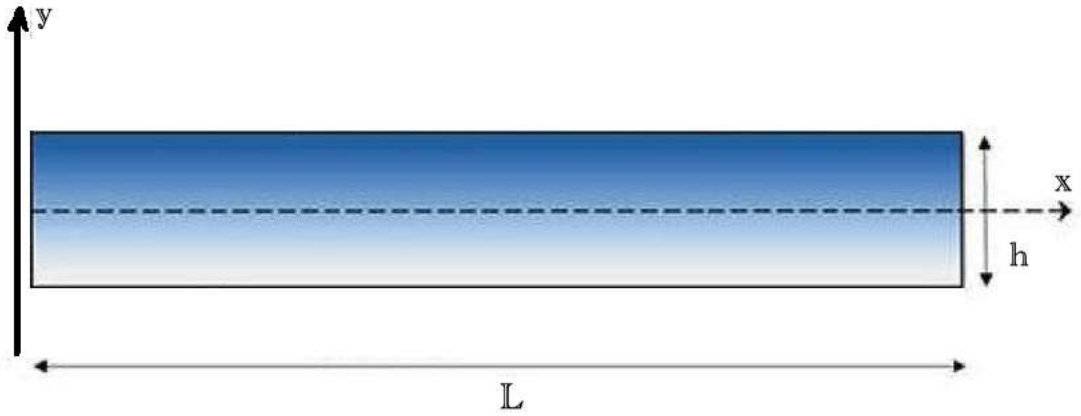

Fig 1. Geometry of the considered thermoelectric structure.

2. Formulation of the problem

A Cartesian coordinate system for a 2D functionally graded magnetic thermoelectric structure with thickness of h and length L as shown in Fig. 1. It is assumed to be subjected to an electric potential $\Phi(x, z, t)$ along the 0x direction and placed in an external constant magnetic field H_0 within the region $R = \{0 < x < L, 0 < y < h\}$ which bounded by boundary S, where S_i $(i = 1, 2, 3, 4)$ are subsets of S such that $S_1 + S_2 = S_3 + S_4 = S$.

The governing equations for fractional order three-temperature nonlinear generalized thermoelastic problems of functionally graded magnetic thermoelectric materials can be written as [22]

$$\sigma_{ij,j} + \mu_0(x+1)^m \varepsilon_{ijk} J_k H_j = \rho(x+1)^m \ddot{u}_i \tag{1}$$

where

$$\sigma_{ij} = (x+1)^m \left[C_{ijkl}\ e\delta_{ij} + \breve{\alpha}\left(u_{j,i} - \varepsilon_{ijk}\omega_k\right) - \beta_{ij}\left(\theta + \tau_1\dot{\theta}\right)\right] \tag{2}$$

$$J_i = \sigma_0\left(E_i + \varepsilon_{ijk}\dot{u}_k B_j - k_0 T_{,i}\right) \tag{3}$$

$$B_i = \mu_0 H_i \tag{4}$$

The fractional order three-temperature radiative heat conduction equations coupled with electron, ion and phonon temperatures can be expressed as

$$D_\tau^a T_\alpha(r,\tau) = \xi\nabla[\mathbb{K}_\alpha\ \nabla T_\alpha(r,\tau)] + \xi\overline{\mathbb{W}}(r,\tau), \xi = \frac{1}{c_\alpha \rho \delta_1} \tag{5}$$

where

$$\overline{\overline{\mathbb{W}}}(r,\tau)=\begin{cases}-\rho\,\mathbb{W}_{ei}\,(T_e-T_i)-\rho\,\mathbb{W}_{ep}\,(T_e-T_p)+\overline{\overline{\mathbb{W}}}(r,\tau), & \alpha=e,\delta_1=1\\ \rho\,\mathbb{W}_{ei}\,(T_e-T_i)+\overline{\overline{\mathbb{W}}}(r,\tau), & \alpha=i,\ \delta_1=1\\ \rho\,\mathbb{W}_{ep}\,(T_e-T_p)+\overline{\overline{\mathbb{W}}}(r,\tau), & \alpha=p,\delta_1=\dfrac{4}{\rho}T_p^3\end{cases} \quad (6)$$

in which

$$\overline{\overline{\mathbb{W}}}(r,\tau)=-\delta_{2j}\mathbb{K}_\alpha\,\dot{T}_{\alpha,ab}+\beta_{ab}T_{\alpha 0}\left[\mathring{A}\delta_{1j}\ddot{u}_{a,b}+\left(\tau_0+\delta_{2j}\right)\ddot{u}_{a,b}\right]$$

$$+\rho c_\alpha\left[\left(\tau_0+\delta_{1j}\tau_2+\delta_{2j}\right)\ddot{T}_\alpha\right]-\rho\,\pi_0\,J_{i,j}$$

and

$$\mathbb{W}_{ei}=\rho\mathbb{A}_{ei}T_e^{-2/3},\qquad \mathbb{W}_{ep}=\rho\mathbb{A}_{ep}T_e^{-1/2},\qquad \mathbb{K}_\alpha=\mathbb{A}_\alpha T_\alpha^{5/2},\alpha=e,i,\qquad \mathbb{K}_p=\mathbb{A}_p T_p^{3+\mathbb{B}} \quad (7)$$

The total energy of a unit mass can be described as follows:

$$P=P_e+P_i+P_p,P_e=c_eT_e,P_i=c_iT_i,P_p=\frac{1}{\rho}c_pT_p^4 \quad (8)$$

Initial and boundary conditions can be written as

$$T_\alpha(x,y,0)=T_\alpha^0(x,y)=g_1(x,\tau) \quad (9a)$$

$$\mathbb{K}_\alpha\frac{\partial T_\alpha}{\partial n}\Big|_{\Gamma_1}=0,\alpha=e,i,T_p\big|_{\Gamma_1}=g_2(x,\tau) \quad (9b)$$

$$\mathbb{K}_\alpha\frac{\partial T_\alpha}{\partial n}\Big|_{\Gamma_2}=0,\alpha=e,i,p \quad (9c)$$

3. BEM simulation for temperature field

The boundary element method is used in this section to solve the nonlinear time-dependent two dimensions three temperature (2D-3T) radiation diffusion equations that are coupled by electron, ion, and photon temperatures.

According to finite difference scheme of Caputo at times $(f+1)\Delta\tau$ and $f\Delta\tau$, we obtain [23]

$$D_\tau^a T_\alpha^{f+1} + D_\tau^a T_\alpha^f \approx \sum_{j=0}^{k} W_{a,j}\left(T_\alpha^{f+1-j}(r) - T_\alpha^{f-j}(r)\right), (f = 1, 2, \dots., F) \quad (10)$$

where

$$W_{a,0} = \frac{(\Delta\tau)^{-a}}{\Gamma(2-a)}, W_{a,j} = W_{a,0}((j+1)^{1-a} - (j-1)^{1-a}), j = 1, 2, \dots., F \quad (11)$$

Based on equation (10), the fractional order heat equations (5) can be replaced by the following system

$$\begin{aligned} &W_{a,0}T_\alpha^{f+1}(r) - \mathbb{K}_\alpha(x)T_{\alpha,II}^{f+1}(r) - \mathbb{K}_{\alpha,I}(x)T_{\alpha,I}^{f+1}(r) \\ &= W_{a,0}T_\alpha^{f}(r) - \mathbb{K}_\alpha(x)T_{\alpha,II}^{f}(r) - \mathbb{K}_{\alpha,I}(x)T_{\alpha,J}^{f}(r) \\ &\quad - \sum_{j=1}^{f} W_{a,j}\left(T_\alpha^{f+1-j}(r) - T_\alpha^{f-j}(r)\right) + \overline{\mathbb{W}}_m^{f+1}(x,\tau) \\ &\quad + \overline{\mathbb{W}}_m^{f}(x,\tau), f = 0, 1, 2, \dots, F \end{aligned} \quad (12)$$

Based on the fundamental solution of (12), the direct formulation of boundary integral equation corresponding to (5) can be expressed as

$$CT_\alpha = \frac{D}{\mathbb{K}_\alpha}\int_O^\tau \int_S [T_\alpha q^* - T_\alpha^* q]\, dS\, d\tau + \frac{D}{\mathbb{K}_\alpha}\int_O^\tau \int_R b\, T_\alpha^*\, dR\, d\tau + \int_R T_\alpha^i T_\alpha^*\big|_{\tau=0}\, dR \quad (13)$$

which can be written in the absence of internal heat sources as follows

$$CT_\alpha = \int_S [T_\alpha q^* - T_\alpha^* q]\, dS - \int_R \frac{\mathbb{K}_\alpha}{D}\frac{\partial T_\alpha^*}{\partial \tau} T_\alpha\, dR \quad (14)$$

We assume that the time derivative of temperature can be approximated by a series of known functions in order to transform the domain integral in (14) to the boundary. $f^j(r)$ and unknown coefficients $a^j(\tau)$ as

$$\frac{\partial T_\alpha}{\partial \tau} \cong \sum_{j=1}^{N} f^j(r)^j a^j(\tau) \quad (15)$$

Also, we assume that $\hat{T}_\alpha^j$ is a solution of

$$\nabla^2 \hat{T}_\alpha^j = f^j \quad (16)$$

Thus, equation (14) results in the following boundary integral equation

$$C\,T = \int_S [T_\alpha q^* - T_\alpha^* q]\, dS + \sum_{j=1}^{N} a^j(\tau) D^{-1}\left(C\hat{T}_\alpha^j - \int_S \left[T_\alpha^j q^* - \hat{q}^j T_\alpha^*\right] dS\right) \quad (17)$$

where

$$\hat{q}^j = -\mathbb{K}_\alpha \frac{\partial \hat{T}_\alpha^j}{\partial n} \tag{18}$$

and

$$a^j(\tau) = \sum_{i=1}^{N} f_{ji}^{-1} \frac{\partial T(r_i, \tau)}{\partial \tau} \tag{19}$$

In which the entries of f_{ji}^{-1} are the coefficients of F^{-1} with matrix F defined as [34]

$$\{F\}_{ji} = f^j(r_i) \tag{20}$$

Using the standard boundary element discretization scheme for equation (17) and using equation (19), we obtain the following set of ordinary differential equations

$$C\,\dot{T}_\alpha + H\,T_\alpha = G\,Q \tag{21}$$

where matrices H and G are depending on the current time step, boundary geometry and material properties, T_α and Q are, respectively, temperature and heat flux vectors at boundary nodes, and b is the internal heat generation vector

The diffusion matrix can be defined as

$$C = -\left[H\,\hat{T}_\alpha - G\,\hat{Q}\right]F^{-1}D^{-1} \tag{22}$$

with

$$\left\{\hat{T}\right\}_{ij} = \hat{T}^j(x_i) \tag{23}$$

$$\left\{\hat{Q}\right\}_{ij} = \hat{q}^j(x_i) \tag{24}$$

In order to solve equation (21) numerically the functions T_α and q are interpolated as

$$T_\alpha = (1-\theta)\,T_\alpha^m + \theta\,T_\alpha^{m+1} \tag{25}$$

$$q = (1-\theta)q^m + \theta\,q^{m+1} \tag{26}$$

where the parameter $\theta = \frac{\tau - \tau^m}{\tau^{m+1} - \tau^m}$, $0 \le \theta \le 1$ determines the practical time τ in the present time step.

By differentiating equation (25) with respect to time we get

$$\dot{T}_\alpha = \frac{dT_\alpha}{d\theta}\frac{d\theta}{d\tau} = \frac{T_\alpha^{m+1} - T_\alpha^m}{\tau^{m+1} - \tau^m} = \frac{T_\alpha^{m+1} - T_\alpha^m}{\Delta\tau^m} \tag{27}$$

By substituting from Equations (25) - (27) into Equation (21), we obtain

$$\left(\frac{C}{\Delta\tau^m} + \theta H\right)T_\alpha^{m+1} - \theta G Q^{m+1} = \left(\frac{C}{\Delta\tau^m} - (1-\theta)H\right)T_\alpha^m + (1-\theta)GQ^m \tag{28}$$

By using initial and boundary conditions at $\Delta\tau^m$ and considering the previous time step solution as initial values for the next step, we obtain the following linear algebraic system

$$\mathbb{a}\mathrm{X} = \mathbb{b} \tag{29}$$

where $\mathbb{a}$ is unknown matrix, and X and $\mathbb{b}$ are known matrices

4. BEM simulation for displacement and microrotation fields

Using the weighted residual method, the governing equations (1) and (2) can be transformed into the following integral equations

$$.\int_R \left(\sigma_{ij,j} + U_i\right) u_i^*\, dR = 0 \tag{30}$$

in which

$$U_i = \mu_0(x+1)^m \varepsilon_{ijk} J_k H_j - \rho \ddot{u}_i \tag{31}$$

The boundary conditions are

$$u_i = \bar{u}_i \qquad \text{on } S_1 \tag{32}$$

$$\lambda_i = \sigma_{ij} n_j = \bar{\lambda}_i \qquad \text{on } S_2 \tag{33}$$

The integration of the first term of equations (33) and (34) leads to

$$-\int_R \sigma_{ij}\, u_{i,j}^*\, dR + \int_R U_i\, u_i^*\, dR = -\int_{S_2} \lambda_i\, u_i^*\, dS \tag{34}$$

According to Huang and Liang [25], the boundary integral equation can be written as

$$-\int_R \sigma_{ij,j}\, u_i^*\, dR + \int_R U_i\, u_i^*\, dR = \int_{S_2} \left(\lambda_i - \bar{\lambda}_i\right) u_i^*\, dS + \int_{S_1} (\bar{u}_i - u_i)\, \lambda_i^*\, dS \tag{35}$$

The integration of (35)'s left-hand side by parts results in

$$-\int_R \sigma_{ij}\, \varepsilon_{ij}^*\, dR + \int_R U_i\, u_i^*\, dR = -\int_{S_2} \bar{\lambda}_i\, u_i^*\, dS - \int_{S_1} \lambda_i\, u_i^*\, dS + \int_{S_1} (\bar{u}_i - u_i)\, \lambda_i^*\, dS \tag{36}$$

According to Eringen [26], the elastic stress can be written as

$$\sigma_{ij} = \mathbb{A}_{ijkl}\, \varepsilon_{kl}, \text{where } \mathbb{A}_{ijkl} = \mathbb{A}_{klij} \tag{37}$$

Hence, equation (36) may be expressed as

$$-\int_R \sigma_{ij}^*\, \varepsilon_{ij}\, dR + \int_R U_i\, u_i^*\, dR = -\int_{S_2} \bar{\lambda}_i\, u_i^*\, dS - \int_{S_1} \lambda_i\, u_i^*\, dS + \int_{S_1} (\bar{u}_i - u_i)\, \lambda_i^*\, dS \tag{38}$$

By applying the integration by parts again to the left-hand side of (38), we obtain

$$\int_R \sigma^*_{ij,j}\, u_i\, dR = -\int_S u^*_i\, \lambda_i\, dS + \int_S \lambda^*_i\, u_i\, dS \tag{39}$$

where

$$\sigma^*_{lj,j} + \Delta^n e_l = 0 \tag{40}$$

According to Dragos [27], the fundamental solution may be written as

$$u^*_i = u^*_{li}\, e_l, \qquad \lambda^*_i = \lambda^*_{li}\, e_l, \tag{41}$$

The weighting functions for $U_i = 0$ and $V_i = \Delta^n$ may be expressed as follows:

$$\sigma^{**}_{ij,j} = 0 \tag{42}$$

On the basis of Dragos [27], the fundamental solution may be expressed as

$$u^*_i = u^{**}_{li}\, e_l, \qquad \lambda^*_i = \lambda^{**}_{li}\, e_l \tag{43}$$

Using the above two sets of weighting functions into (39) we have

$$C^n_{li} u^n_i = -\int_S \lambda^*_{li}\, u_i\, dS + \int_S u^*_{li}\, \lambda_i\, dS \tag{44}$$

$$C^n_{li} \omega^n_i = -\int_S \lambda^{**}_{li}\, u_i\, dS + \int_S u^{**}_{li}\, \lambda_i\, dS \tag{45}$$

Thus, we obtain

$$C^n \mathbb{q}^n = -\int_S \mathbb{p}^*\, \mathbb{q}\, dS + \int_S \mathbb{q}^*\, \mathbb{p}\, dS \tag{46}$$

in which

$$C^n = \begin{bmatrix} C_{11} & C_{12} \\ C_{21} & C_{22} \end{bmatrix}, \mathbb{q}^* = \begin{bmatrix} u^*_{11} & u^*_{12} \\ u^*_{21} & u^*_{22} \end{bmatrix}, \mathbb{p}^* = \begin{bmatrix} \lambda^*_{11} & \lambda^*_{12} \\ \lambda^*_{21} & \lambda^*_{22} \end{bmatrix}, \mathbb{q} = \begin{bmatrix} u_1 \\ u_2 \end{bmatrix}, \mathbb{p} = \begin{bmatrix} \lambda_1 \\ \lambda_2 \end{bmatrix} \tag{47}$$

Now, we introduce the following relations

$$\mathbb{q} = \psi\, \mathbb{q}^j, \mathbb{p} = \psi\, \mathbb{p}^j \tag{48}$$

By discretizing the boundary, we can write (46) as

$$C^n \mathbb{q}^n = \sum_{j=1}^{N_e} \left[-\int_{\Gamma_j} \mathbb{p}^*\, \psi\, d\Gamma \right] \mathbb{q}^j + \sum_{j=1}^{N_e} \left[\int_{\Gamma_j} \mathbb{q}^*\, \psi\, d\Gamma \right] \mathbb{p}^j \tag{49}$$

Which can be expressed as

$$C^i \mathbb{q}^i = -\sum_{j=1}^{N_e} \widehat{\mathbb{H}}^{ij}\, \mathbb{q}^j + \sum_{j=1}^{N_e} \widehat{\mathbb{G}}^{ij} \mathbb{p}^j \tag{50}$$

By employing the following formula

$$\mathbb{H}^{ij} = \begin{cases} \widehat{\mathbb{H}}^{ij} & if\ \ i \neq j \\ \widehat{\mathbb{H}}^{ij} + C^i & if\ \ i = j \end{cases} \tag{51}$$

Hence, equation (50) may be expressed as

$$\sum_{j=1}^{N_e} \mathbb{H}^{ij}\, \mathbb{q}^{j} = \sum_{j=1}^{N_e} \widehat{\mathbb{G}}^{ij}\, \mathbb{p}^{j} \tag{52}$$

The global matrix system equation for all i nodes can be written as follows

$$\mathbb{H}\mathbb{Q} = \mathbb{G}\mathbb{P} \tag{53}$$

where $\mathbb{Q}$ denotes the displacements and $\mathbb{P}$ denotes the tractions.

Now, we can write (53) into the following form

$$\mathbb{A}\,\mathbb{X} = \mathbb{B} \tag{54}$$

In Matlab (R2018a), an explicit staggered predictor-corrector scheme based on the communication-avoiding generalized minimal residual (CA-GMRES) method is efficiently implemented for solving the resulting simultaneous linear algebraic systems to obtain the temperature and displacement fields [28].

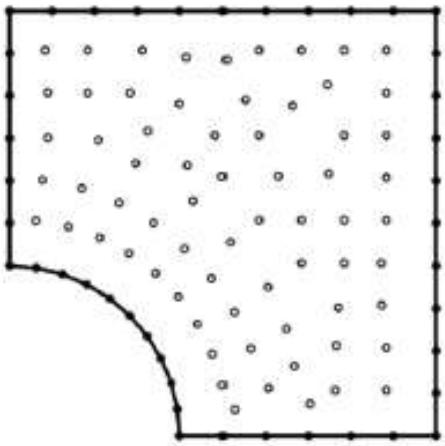

Fig. 2. Boundary element model of the considered structure.

5. Numerical results and discussion

In the context of functionally graded magnetic thermoelectric materials, the proposed BEM technique can be applied to a wide range of fractional-order nonlinear generalised thermal stress problems. The BEM discretization was performed using 42 boundary elements and 68 internal points, as shown in Fig. 2.

Fig. 3. Shows the variation of the thermal stress σ_{11} along x-axis for different values of fractional order parameter ($a = 0.3, 0.6\ and\ 0.9$). It is shown from this figure that the thermal stress σ_{11}

decreases with the increase of x until $x = 0.9$. Then it increases with the increase of x. It is also shown from this figure that the thermal stress σ_{11} decreases with the increase of fractional order parameter.

Fig. 4. Shows the variation of the thermal stress σ_{12} along x-axis for different values of fractional order parameter ($a = 0.3, 0.6\ and\ 0.9$). It is shown from this figure that the thermal stress σ_{12} decreases with the increase of x. It is also shown from this figure that the thermal stress σ_{21} increases with the increase of fractional order parameter.

Fig. 5 Shows the variation of the thermal stress σ_{22} along x-axis for different values of fractional order parameter ($a = 0.3, 0.6\ and\ 0.9$). It is shown from this figure that the thermal stress σ_{22} increases with the increase of x. It is also shown from this figure that the thermal stress σ_{22} decreases with the increase of fractional order parameter.

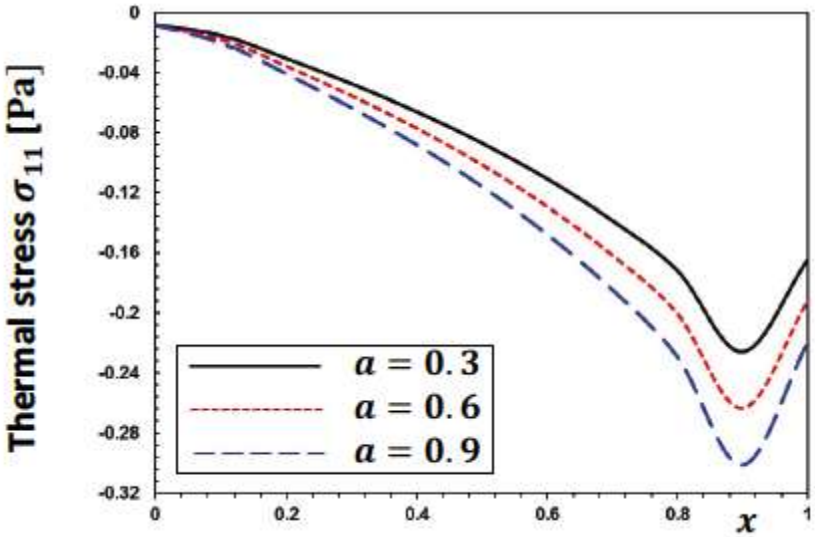

Fig. 3. Variation of the thermal stress σ_{11} along x-axis for different values of fractional order parameter.

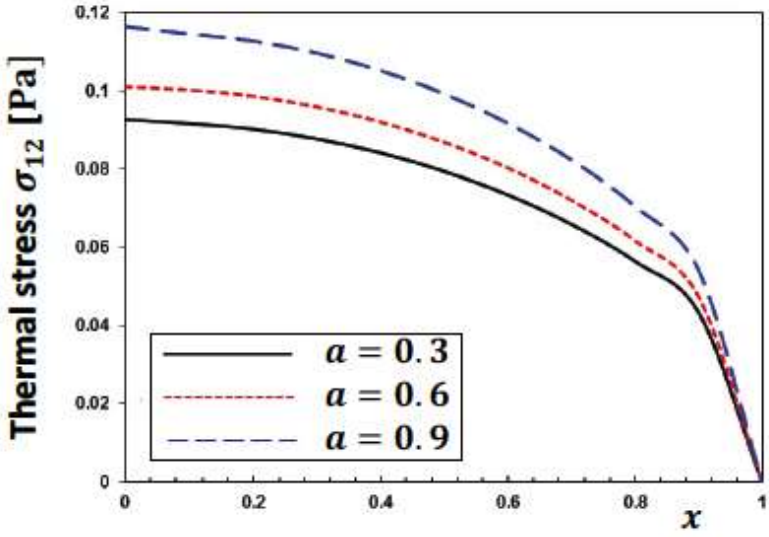

Fig. 4. Variation of the thermal stress σ_{12} along x-axis for different values of fractional order parameter.

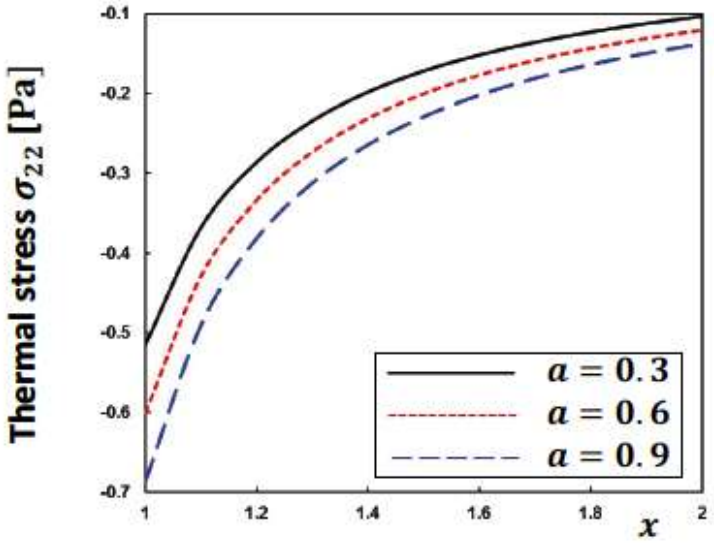

Fig. 5. Variation of the thermal stress σ_{22} along x-axis for different values of fractional order parameter.

Fig. 6. Shows the variation of the thermal stress σ_{11} along x-axis for different values of functionally graded parameter ($m = 0.3, 0.6\ and\ 0.9$). It is shown from this figure that the thermal stress σ_{11} increases with the increase of x until $x = 0.9$. Then it decreases with the increase of x. It is also shown from this figure that the thermal stress σ_{11} increases with the increase of functionally graded parameter.

Fig. 7. Shows the variation of the thermal stress σ_{12} along x-axis for different values of functionally graded parameter ($m = 0.3, 0.6\ and\ 0.9$). It is shown from this figure that the thermal stress σ_{12} increases with the increase of x. It is also shown from this figure that the thermal stress σ_{21} decreases with the increase of functionally graded parameter.

Fig. 8 Shows the variation of the thermal stress σ_{22} along x-axis for different values of functionally graded parameter ($m = 0.3, 0.6\ and\ 0.9$). It is shown from this figure that the thermal stress σ_{22} increases with the increase of x. It is also shown from this figure that the thermal stress σ_{22} decreases with the increase of functionally graded parameter.

It is noted from figures 3-8 that the fractional order parameter and functionally graded parameter have a strong effect on the thermal stress σ_{11}, σ_{12} and σ_{22} in the functionally graded magnetic thermoelectric materials.

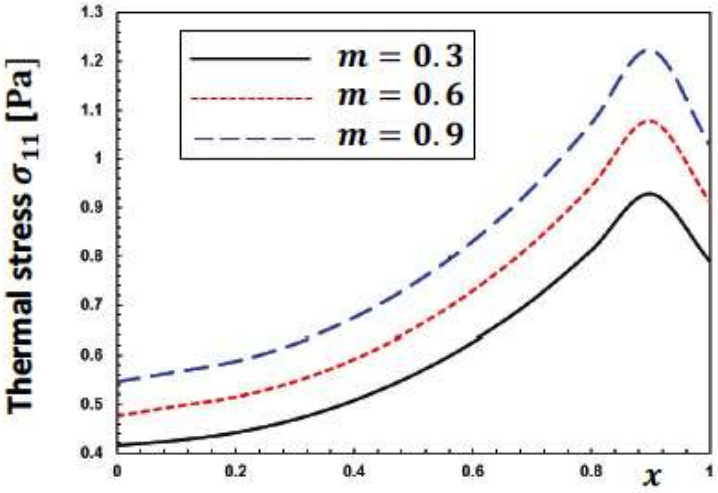

Fig. 6. Variation of the thermal stress σ_{11} along x-axis for different values of functionally graded parameter.

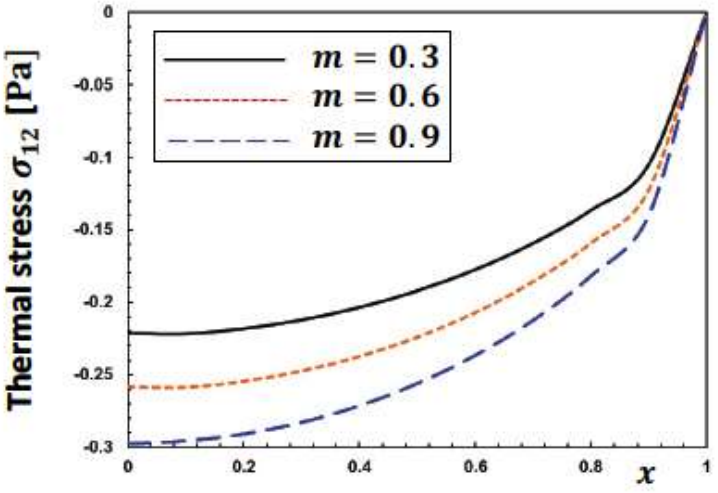

Fig. 7. Variation of the thermal stress σ_{12} along x-axis for different values of functionally graded parameter.

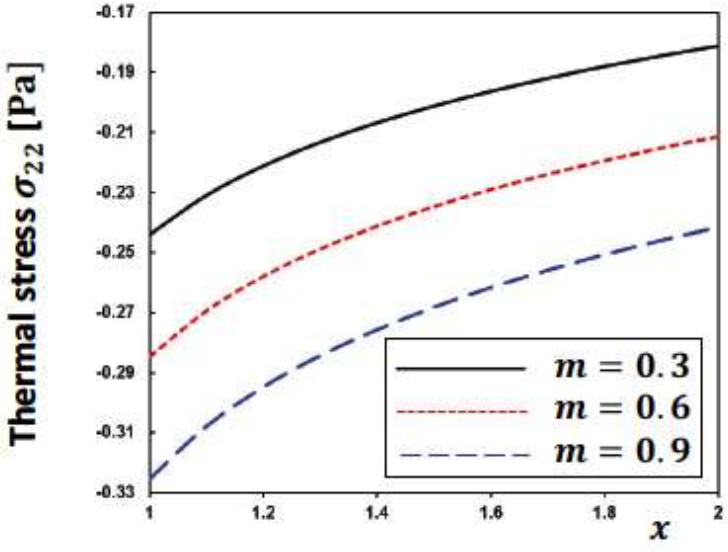

Fig. 8. Variation of the thermal stress σ_{22} along x-axis

for different values of functionally graded parameter.

There were no published results to demonstrate the validity of the proposed technique's results. Some literatures, on the other hand, can be regarded as special cases of the considered general study. Figure 9 shows the variation of the special case thermal stress σ_{11} along x-axis for BEM, FEM and NMM in the case of fractional order ($a = 0.6$) homogeneous ($m = 0.0$). Fig. 10 shows the propagation of the thermal stress σ_{11} along x-axis for BEM, FEM and NMM in the case of zero fractional order, ($a = 0.0$) and non-homogeneous ($m = 0.6$). These findings for thermal stress σ_{11} in functionally graded magnetic thermoelectric materials, show that the BEM findings are in a very good agreement with the FEM findings of Prajwal and Bhat [29], and NMM findings of Singh [30]. These results show that the BEM results are in a very good agreement to the FEM and NMM results. Thus, the validity of the proposed technique was confirmed.

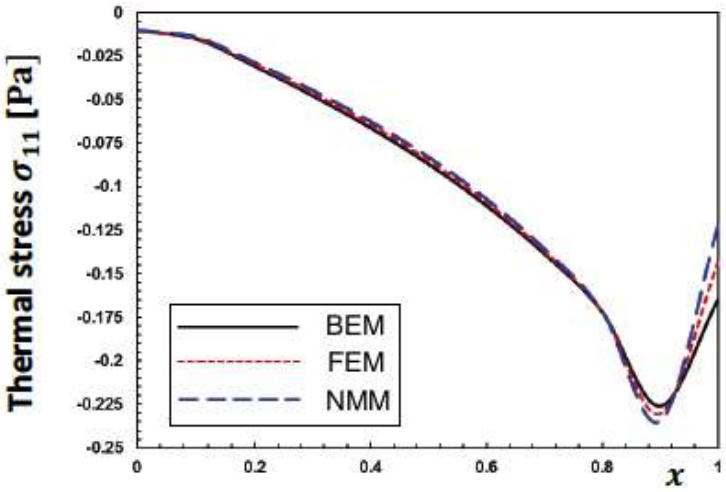

Fig. 9. Variation of the special case thermal stress σ_{11} along x-axis for BEM, FEM and NMM ($a = 0.6, m = 0.0$).

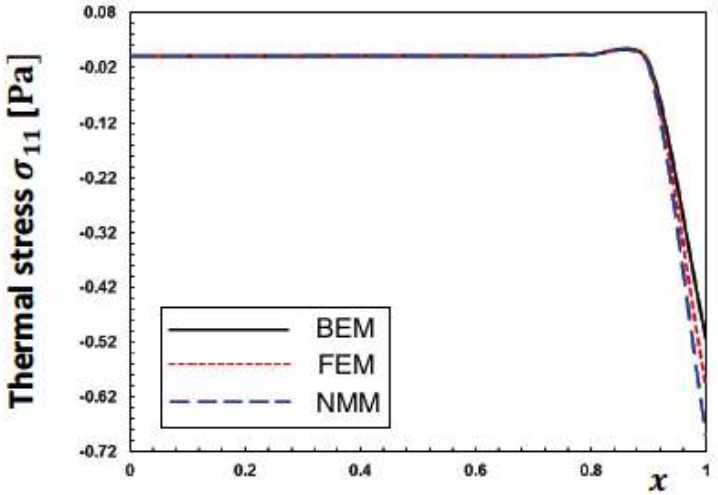

Fig. 10. Variation of the special case thermal stress σ_{11} along x-axis for BEM, FEM and NMM ($a = 0.0, m = 0.6$).

6. Conclusion

Based on an explicit staggered predictor-corrector scheme The primary goal of this paper is to present a novel fractional-order theory that will aid in the advancement of functionally graded magnetic thermoelectric materials' technological and industrial applications. Three-temperature nonlinear generalized thermoelasticity of functionally graded magnetic thermoelectric materials is the name given to this theory (FGMTMs). We must successfully adopt computerized numerical methods for solving and simulating complex nonlinear FGM problems in order to successfully guide the current research field toward the development of new functionally graded materials (FGMs). The governing equations are extremely difficult to solve experimentally or analytically due to the proposed theory's severe nonlinearity. To address this issue, new numerical approaches for solving such equations must be developed. We propose a new formulation of the boundary element method for solving the theory's governing equations (BEM). Because of the advantages of the BEM approach, such as the ability to deal with issues with complicated shapes that are difficult to deal with using standard methods, and the lack of the need for internal domain discretization. It also necessitates low CPU utilization and memory storage. As a result, the BEM is appropriate for a wide variety of sophisticated FGMTMs applications. The numerical results are discussed, with an emphasis on the effects of magnetic fields and graded parameters on thermal stresses in FGMTMs. Both the proposed formulation and solution technique are supported by the numerical results.

References

1. [1] Knopoff L. The interaction between elastic wave motions and a magnetic field in electrical conductors. J Geophys Res 1955;60:441–56.
2. [2] Chadwick P. Thermoelasticity. The dynamical theory, progress in solid mechanics, Vol 1. Amsterdam: North-Holland Publishing Co; 1960. MR 0113406 p. 263–328.
3. [3] Kaliski S, Petykiewicz J. Equation of motion coupled with the field of temperature in a magnetic field involving mechanical and electrical relaxation for anisotropic bodies. Proc Vib Probl 1959;1:3–11.
4. [4] Rajagopal, K.R.; Ružička, M. Mathematical modeling of electrorheological materials, Continuum Mech. Thermodyn. 2001, 13, 59–78.
5. [5] Brigadnov, I.A.; Dorfmann, A. Mathematical modeling of magnetorheological fluids, Continuum Mech. Thermodyn. 2005, 17, 29–42.
6. [6] Dorfmann, A.; Ogden, R.W. Magnetoelastic modelling of elastomers, Euro. J. Mech. A/Solids 2000, 22, 497–507.
7. [7] Carlson, J.D.; Jolly, M.R.; MR fluid, foam and elastomer devices, Mechatronics 10 (2000) 555–569.
8. [8] Wineman, A.S.; Rajagopal, K.R. On constitutive equations for electrorheological materials, Continuum Mech. Thermdynam. 7, 1–22.
9. [9] Rigbi, Z.; Jilkén L. The response of an elastomer filled with soft ferrite to mechanical and magnetic in puences, J. Magn. Magn. Mater. 37 (1983) 67–276.

10. [10] Ginder J.M. Rheology controlled by magnetic fields, Encyl. Appl. Phys. 16 (1996) 487–503.
11. [11] Kankanala, S.V.; Triantafyllidis N.J. On finitely strained magnetorheological elastomers, Mech. Phys. Solids 52 (2004) 2869–2908.
12. [12] Ezzat, M.A.; Awad, E.S. Micropolar generalized magneto-thermoelasticity with modified Ohm's and Fourier's laws, J. Math. Anal. Appl. 353 (2009) 99–
13. 113.
14. [13] Fahmy M.A. (2021). A novel BEM for modeling and simulation of 3T nonlinear generalized anisotropic micropolar-thermoelasticity theory with memory dependent derivative. CMES-Computer Modeling in Engineering & Sciences. Volume 126, pp. 175-199.
15. [14] Fahmy M.A. (2021). A new boundary element formulation for modeling and simulation of three-temperature distributions in carbon nanotube fiber reinforced composites with inclusions. Mathematical Methods in the Applied Science. DOI: https://doi.org/10.1002/mma.7312
16. [15] Fahmy M.A. (2020). Boundary element algorithm for nonlinear modeling and simulation of three temperature anisotropic generalized micropolar piezothermoelasticity with memory-dependent derivative. International Journal of Applied Mechanics, Volume 12, pp. 2050027.
17. [16] Fahmy MA, Shaw S, Mondal S, Abouelregal AE, Lotfy Kh., Kudinov IA, Soliman AH (2021). Boundary Element Modeling for Simulation and Optimization of Three-Temperature Anisotropic Micropolar Magneto-thermoviscoelastic Problems in Porous Smart Structures Using NURBS and Genetic Algorithm. International Journal of Thermophysics. vol. 42, pp. 29.
18. [17] Fahmy M.A. (2021). Boundary element modeling of 3T nonlinear transient magneto-thermoviscoelastic wave propagation problems in anisotropic circular cylindrical shells, Composite Structures vol. 27, pp. 114655. https://doi.org/10.1016/j.compstruct.2021.114655
19. [18] Fahmy M.A. (2021). A new boundary element algorithm for a general solution of nonlinear space-time fractional dual-phase-lag bio-heat transfer problems during electromagnetic radiation. Case Studies in Thermal Engineering, vol. 25, pp. 100918. DOI: https://doi.org/10.1016/j.csite.2021.100918
20. [19] Fahmy M.A. (2021). A new boundary element algorithm for modeling and simulation of nonlinear thermal stresses in micropolar FGA composites with temperature-dependent properties. Advanced Modeling and Simulation in Engineering Sciences, vol. 8, pp. 1-23. https://doi.org/10.1186/s40323-021-00193-6
21. [20] Fahmy M.A. (2021). A New BEM for Fractional Nonlinear Generalized Porothermoelastic Wave Propagation Problems. CMC- Computers, Materials and Continua, vol. 68, no.1, pp. 59-76. DOI:10.32604/cmc.2021.015115
22. [21] Fahmy M.A. (2021). A New BEM Modeling Algorithm for Size-Dependent Thermopiezoelectric Problems in Smart Nanostructures. CMC-Computer, Materials & Continua vol. 69, no. 1, pp. 931-944. https://doi.org/10.32604/cmc.2021.018191
23. [22] Fahmy M.A. Implicit–explicit time integration DRBEM for generalized magneto-ther- moelasticity problems of rotating anisotropic viscoelastic functionally graded solids. Eng Anal Bound Elem 2013;37:107–15.
24. [23] C. Cattaneo, Sur une forme de i'equation de la chaleur elinant le paradox d'une propagation instantanc. Comptes rendus de l'Académie des Sciences, Paris: Gauthier-Villars 1958; 247: 431-433.
25. [24] Fahmy M.A. Computerized boundary element solutions for thermoelastic problems: applications to functionally graded anisotropic structures. Saarbrücken, Germany: LAP Lambert Academic Publishing; 2017.

26. [25] Huang FY,Liang KZ. Boundary element method for micropolar thermoelasticity.Eng Anal Bound Elem 1996;17:19–26.
27. [26] Eringen AC. Theory of micropolar elasticity. Fracture, II. Edited by. New York: Aca- demic Press; 1968.
28. [27] Dragos L. Fundamental solutions in micropolar elasticity. Int J Eng Sci 1984;22:265–75.
29. [28] Fahmy M.A. A new boundary element strategy for modeling and simulation of three temperatures nonlinear generalized micropolar-magneto-thermoelastic wave propagation problems in FGA structures. Engineering Analysis with Boundary Elements 2019, 108, 192-200. DOI: 10.1016/j.enganabound.2019.08.006
30. [29] Prajwal, K.T.; Bhat, P. Thermal analysis of a Thermoelectric Generator (TEG) using FEM technique. IOP Conf. Ser.: Mater. Sci. Eng. 2021, 1045, 012018 doi:10.1088/1757-899X/1045/1/012018
31. [30] Singh, J. Synthesis and Characterization of Some Useful Thermoelectric Materials. Asian Journal of Chemistry 2019, 31, 633-636

Availability of Data and Materials

All data generated or analysed during this study are included in this published article